

Rigorous Analysis of Software Countermeasures against Cache Attacks

Goran Doychev
IMDEA Software Institute
 goran.doychev@imdea.org

Boris Köpf
IMDEA Software Institute
 boris.koepf@imdea.org

Abstract

CPU caches introduce variations into the execution time of programs that can be exploited by adversaries to recover private information about users or cryptographic keys.

Establishing the security of countermeasures against this threat often requires intricate reasoning about the interactions of program code, memory layout, and hardware architecture and has so far only been done for restricted cases.

In this paper we devise novel techniques that provide support for bit-level and arithmetic reasoning about pointers in the presence of dynamic memory allocation. These techniques enable us to perform the first rigorous analysis of widely deployed software countermeasures against cache attacks on modular exponentiation, based on executable code.

1 Introduction

CPU caches reduce the latency of memory accesses on average, but not in the worst case. Thus, they introduce variations into the execution time that can be exploited by adversaries to recover secrets from programs, such as private information about users or cryptographic keys [5, 28, 1, 30, 15, 37]. A large number of techniques have been proposed to counter this threat. Some proposals work at the level of the operating system [13, 19, 40], others at the level of the hardware architecture [14, 35, 34] or the cryptographic protocol [12]. In practice, however, software countermeasures are often the preferred choice because they can be easily deployed.

The most defensive countermeasure is to ensure that control flow, memory accesses, and execution time of individual instructions do not depend on secret data. While such code is easily seen to prevent leaks through instruction and data caches, hiding all dependencies can come with performance penalties caused, for example,

by dummy memory accesses [25, 8].

More permissive countermeasures are to ensure that both branches of each conditional fit into a single line of the instruction cache, to preload lookup tables, or to permit secret-dependent memory access patterns as long as they are secret-*independent* at the granularity of cache lines or sets. Such permissive code can be faster and is widely deployed in crypto-libraries such as OpenSSL. However, analyzing its security requires intricate reasoning about the interactions of the program and the hardware platform and has so far only been done for restricted cases.

A major hurdle for reasoning about these interactions are the requirements put on tracking memory addresses:

- On one hand, static analysis of dynamic memory allocation requires memory addresses to be dealt with symbolically.
- On the other hand, cache-aware code requires support for accurate tracking of bit-level and arithmetic operations. This is needed for establishing properties of the memory layout, such as alignment of tables with cache line or page boundaries, and for basic pointer arithmetic.

While there are solutions that address each of the requirements in isolation, supporting them together is challenging because the demand for symbolic treatment conflicts with the demand for bit-level precision. In this paper we address this problem by devising a novel techniques that can deal with all requirements at the same time and thus enables the automatic, static analysis of permissive software countermeasures against cache side-channels attacks in executable code.

Specifically, we introduce *masked symbols*, an abstraction that can represent unknown addresses, together with information about some of their bits. Masked symbols encompass unknown addresses as well as known constants; more importantly, they also support intermediate cases, such as addresses that are unknown except for their least significant bits, which are zeroed out to align

with cache line boundaries. We cast arithmetic and bit-level operations on masked symbols in terms of a simple set-based abstract domain, which is a data structure that supports approximating the semantics of programs [10].

The masked symbol abstract domain enables us to reason about security with respect to a wide range of observers of a program execution, most of which are out of scope of existing program analysis techniques. Supported observers include one that can see the trace of accesses to the instruction cache (commonly known as the *program counter security model* [25]) but also weaker ones that can see only the trace of memory blocks or cache banks, with respect to data, instruction, or shared caches. We devise another novel abstract domain that over-approximates the set of observations each of those adversaries can make during a program execution, and that features a counting procedure for quantifying the amount of information they can learn.

We implement our novel techniques on top of the CacheAudit static analyzer [11] and we evaluate their effectiveness in a case study where we perform the first formal analysis of commonly used software countermeasures for protecting modular exponentiation algorithms. The paper contains a detailed description of our case study; here we highlight the following results:

- We analyze the security of the scatter/gather countermeasure used in OpenSSL 1.0.2f for protecting window-based modular exponentiation. Scatter/gather ensures that the pattern of data cache accesses is secret-independent at the level of granularity of cache lines and, indeed, our analysis of the binary executables reports security against adversaries that can monitor only cache line accesses.
 - Our analysis of the scatter/gather countermeasure also reports a leak with respect to adversaries that can monitor memory accesses at a more fine-grained resolution. This weakness that has been exploited in the CacheBleed attack [38], where the adversary observes accesses to the individual banks within a cache line. We analyze the variant of scatter/gather published in OpenSSL 1.0.2g as a response to the attack and prove its security with respect to powerful adversaries that can monitor the full address trace.
 - Our analysis detects the side channel in the square-and-multiply based algorithm in libcrypto 1.5.2 that has been exploited in [37, 22], but can prove the absence of instruction and data cache leaks in the square-and-always-multiply algorithm used in libcrypto 1.5.3, for some compiler optimization levels.
- Overall, our results illustrate (once again) the dependency of software countermeasures against cache attacks on brittle details of the compilation and the hardware architecture, and they demonstrate (for the first time) how automated program analysis can effectively support

the rigorous analysis of permissive software countermeasures.

In summary, our contributions are to devise novel techniques that enable cache-aware reasoning about dynamically allocated memory, and to put these techniques to work in the first rigorous analysis of widely deployed permissive countermeasures against cache side channel attacks.

2 Illustrative Example

We illustrate the scope of the techniques developed in this paper using a problem that arises in implementations of windowed modular exponentiation. There, powers of the base are pre-computed and stored in a table for future lookup. Figure 1 shows an example memory layout of two such pre-computed values p_2 and p_3 , each of 3072 bits, which are stored in heap memory. An adversary that observes accesses to the six memory blocks starting at `80eb140` knows that p_2 was requested, which can give rise to effective key-recovery attacks [22].

80eb140	00 00 00 00 00 00 01 89 66 07 7e bd 53 8d 2f 3e
80eb150	08 e0 7c de 16 09 d1 p2 0 db 1d 94 71 65 ca 35 4b
80eb160	6c 35 61 ac ec 74 80 20 b7 9e e9 76 c0 f1 f9 9a
80eb170	df b3 ac 9d ad fa 98 35 93 c3 5f ef 3c ac f9 df
80eb180	ec 6c 94 45 60 ad 03 e0 7a 03 66 4e 60 17 5d 8b
.....
80eb2b0	0e b7 c1 83 76 09 6d 95 62 20 e2 5b 31 1a 00 d8
80eb2c0	e7 d5 a6 a4 2d 41 2e 55 00 00 00 00 00 01 89
80eb2d0	1f ca 10 9d 92 26 d1 p3 00 aa ca d9 d0 23 bc 94
80eb2e0	b2 ba 4c e6 19 d5 d1 b 44 e6 5b 86 cf c9 3e e8
80eb2f0	de dc cd 46 6d b1 61 6c 4b 58 df 2f ad a6 99 f7
80eb300	86 c1 05 f8 83 89 4a 53 a8 c9 d0 da fd 7f 50 7a
.....
80eb430	7e 61 30 7c c4 10 b3 2a 85 5c fc fb 3c 07 29 86
80eb440	ac 9a 2a 5f 73 c7 80 75 80 68 be 98 0b e3 49 b4

Figure 1: Layout of pre-computed values in main memory, for the windowed modular exponentiation implementation from libcrypto 1.6.1. Black lines denote the memory block boundaries, for an architecture with blocks of 64 bytes.

Defensive approaches for table lookup, as implemented in NaCl or libcrypto 1.6.3, avoid such vulnerabilities by accessing *all* table entries in a constant order. OpenSSL 1.0.2f instead uses a more permissive approach that accesses only *one* table entry, however it uses a smart layout of the tables to ensure that the requested memory blocks are loaded into cache in a constant order. An example layout for storing 8 pre-computed values is shown in Figure 2. The code that manages such tables consists of three functions, which are given in Figure 3.

- To create the layout, the function `align` aligns a buffer with the memory block boundary by ensuring the least-significant bits of the buffer address are zeroed.
- To write a value into the array the function `scatter` ensures that the bytes of the pre-computed values are stored `spacing` bytes apart.

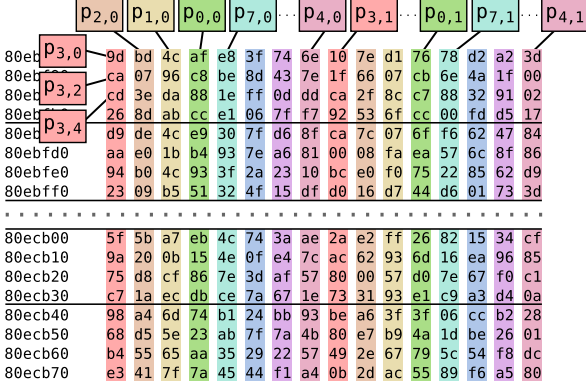


Figure 2: Layout of pre-computed values in main memory, achieved with the scatter/gather countermeasure. Data highlighted in different colors correspond to pre-computed values p_0, \dots, p_7 , respectively. Black lines denote the memory block boundaries, for an architecture with blocks of 64 bytes.

- Finally, to retrieve a pre-computed value from the buffer, the function `gather` assembles the value by accessing its bytes in the same order they were stored.

```

1 align ( buf ):
2     return buf - ( buf & ( block_size - 1 ) ) + block_size
3
4 scatter ( buf, p, k ):
5     for i := 0 to N - 1 do
6         buf [k + i * spacing] := p [k][i]
7
8 gather ( r, buf, k ):
9     for i := 0 to N - 1 do
10        r [i] := buf [k + i * spacing]

```

Figure 3: Scatter/gather method from OpenSSL 1.0.2f for aligning, storing and retrieving pre-computed values.

In this paper, we develop binary analysis techniques which enable the automatic reasoning about the effectiveness of such countermeasures, for a variety of adversaries. Our analysis handles the dynamically-allocated address in `buf` from Figure 3 symbolically, but is still able to establish the effect of `align` by considering bit-level semantics of arithmetic operators on symbols: First, the analysis establishes that `buf & (block_size - 1)` clears the most-significant bits of the symbol s ; second, when subtracting this value from `buf`, the analysis determines that the result is s with the least-significant bits cleared; third, the analysis determines that adding `block_size` leaves the least-significant bits unchanged, but affects the unknown bits, resulting in a new symbol $s' \neq s$ whose least significant bits are cleared.

Using this information, in `gather`, our analysis es-

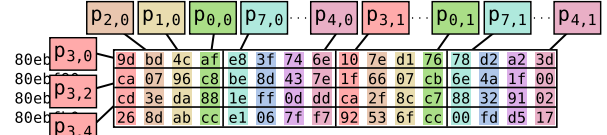


Figure 4: Layout of pre-computed values in cache banks, for a platform with 16 banks of 4-bytes. The shown data fits into one memory block, and the cells of the grid represent the cache banks.

establishes that, independently from the value of k , at each iteration of the loop, the most-significant bits of the accessed location are the same. Combining this information with knowledge about the underlying architecture such as the block size, the analysis establishes that the sequence of accessed memory blocks is the same, thus the countermeasure ensures security of scatter/gather with respect to adversary who makes observations at memory-block granularity.

Our analysis is also able to detect the recently disclosed CacheBleed attack [38], where the adversary can use *cache-bank conflicts* to make finer-grained observations and recover the pre-computed values despite scatter/gather. For example, the pre-computed values in Figure 2 will be distributed to different cache banks as shown in Figure 4, and cache-bank adversaries can distinguish between accesses to p_0, \dots, p_3 and p_4, \dots, p_7 .

3 Memory Trace Adversaries

In this section, we present the adversaries considered in this paper, which are ranked by their observational capabilities. We start by introducing an abstract notion of programs and traces.

3.1 Programs and Traces

We introduce an abstract notion of programs as the transformations of the the main memory and CPU register contents (which we collectively call the *machine state*), caused by the execution of the program’s instructions. Formally, a program $P = (\Sigma, I, \mathcal{A}, \mathcal{T})$ consists of the following components:

- Σ - a set of *states*
- $I \subseteq \Sigma$ - a set of possible *initial states*
- \mathcal{A} - a set of *addresses*
- $\mathcal{T} \subseteq \Sigma \times \mathcal{A}^* \times \Sigma$ - a *transition relation*

An initial state in I captures the inputs to the program. We distinguish between variations in adversary observations that are due to secret (or *high*) data and those that are due to public (or *low*) data. For this, we split the initial state into a low part I_{lo} and a high part I_{hi} , i.e., $I = I_{lo} \times I_{hi}$.

A transition $(\sigma_i, a, \sigma_j) \in \mathcal{T}$ captures two aspects of a computation step: first, it describes how the instruction set semantics operates on data stored in the machine state, namely by updating σ_i to σ_j ; second, it describes the sequence of memory accesses $a \in \mathcal{A}^*$ issued during this update, which includes the addresses accessed when fetching instructions from the code segment, as well as the addresses containing accessed data. To capture the effect of one computation step in presence of unknown inputs, we define the *next* operator: $next(S) = \{t.\sigma_n a_n \sigma_{n+1} \mid t.\sigma_n \in S \wedge (\sigma_n, a_n, \sigma_{n+1}) \in \mathcal{T}\}$.

A *trace* of P is an alternating sequence of states and addresses $\sigma_0 a_0 \sigma_1 a_1 \dots \sigma_n$ such that $\sigma_0 \in I$, and that for all $i \in \{0, \dots, n-1\}$, $(\sigma_i, a_i, \sigma_{i+1}) \in \mathcal{T}$. The set of all traces of P is its *collecting semantics* $Col \subseteq Traces$. In this paper, we only consider terminating programs, and define their collecting semantics as the least fixpoint of the *next* operator containing I : $Col = I \cup next(I) \cup next^2(I) \cup \dots$.

The collecting semantics can be split into a family of collecting semantics Col_λ with $I = \{\lambda\} \times I_{hi}$, one for each $\lambda \in I_{lo}$, such that $Col = \bigcup_{\lambda} Col_\lambda$.

3.2 A Hierarchy of Memory Trace Observers

We define security notions against memory trace attacks, corresponding to different observational capabilities of the adversary. We express these capabilities in terms of *views*, which are functions that map traces in Col to the set of observations an adversary can make. The views can be derived by successively applying lossy transformations to the sequence of memory accesses of a program, which leads to a hierarchy of security definitions.

Granularity of Observations The difference between the considered adversaries is the granularity at which they can observe the sequence of accesses to the main memory. We consider adversaries who can observe accesses at the granularity of *observable units* such as memory pages, cache lines, or cache banks, and cannot distinguish between accesses within the same observable unit. Modern microarchitectures determine the offset within those units from the $b := \log_2 k$ least-significant bits of the memory address, where k is the byte-size of the unit. For example, an architecture with 4KB pages, lines of 64B, and banks of 4B will use bits 0–11 for memory page, 0–5 for cache line, and 0–1 for cache bank offset. This allows defining the adversaries’ observation by projecting out those bits from the memory addresses, i.e., for a 32-bit system, we assume that on access to address a , the adversary observes $\pi_{31:b}(a) := (a_{31}, a_{30}, \dots, a_b)$. The view

of an adversary is defined as $view: \sigma_0 a_0 \sigma_1 a_1 \dots \sigma_n \mapsto \pi_{31:b}(a_0) \pi_{31:b}(a_1) \dots \pi_{31:b}(a_{n-1})$.

Hierarchy of Observers According to the observable units of adversaries, we distinguish between the following observers:

- The *address-trace observer* can observe the full sequence $a_0 a_1 \dots a_{n-1}$ of memory locations that are accessed. Security against this adversary implies resilience to many kinds of microarchitectural side channels, through cache, TLB, DRAM, and branch prediction buffer.¹ An address-trace observer restricted to instruction-addresses is equivalent to the program counter security model [25].

- The *block-trace observer* can observe the sequence of memory blocks loaded by the user into cache. Security against this adversary implies resilience against adversaries that can monitor memory accesses at the level of granularity of cache lines, which are commonly of size $k = 32, 64,$ or 128 bytes. Most known cache-based attacks exploit observations at the granularity of cache lines, e.g. [29, 39, 22].

- The *bank-trace observer* can observe a sequence of accessed cache banks. An example of an attack at the granularity of cache banks is CacheBleed [38] against the scatter/gather implementation from OpenSSL 1.0.2f. The platform targeted in this attack has 16 banks of size $k = 4$ bytes.

- The *page-trace observer* can observe memory accesses at the granularity of accessed memory pages, which are commonly of size $k = 4096$ bytes. Examples of such attacks appear in [36] and [32].

The views of these observers are denoted by $view^{addr}$, $view^{block}$, $view^{bank}$, and $view^{page}$, respectively.

Observations Modulo Stuttering We also consider a class of adversaries that can observe a sequence of memory blocks, but that can only make limited observations about repeated accesses to the same memory block (which we call *stuttering*). This captures that the adversary cannot count the number of executed instructions, as long as they are guaranteed not to access main memory²; it is motivated by the fact that the latency of cache misses dwarfs that of cache hits and is hence easier to observe.

We formalize this intuition in terms of a function $view^{bblock}$ that takes as input a sequence w of blocks and maps maximal subsequences b^r to the block b . That is, repetitions of any block are removed.

¹We do not model, or make assertions about, the influence of advanced features such as out-of-order-execution.

²Here we rely on the (weak) assumption that the second b in any access sequence $\dots bb \dots$ is guaranteed to hit the cache.

Example 1. The function view^{bblock} maps both *aabccddc* and *abbbccddcc* to the sequence *abcdc*, making them indistinguishable to the adversary.

4 Static Quantification of Leaks

In this section we characterize the amount of information leaked by a program, and we show how this amount can be over-approximated by static analysis. While the basic idea is standard, our presentation differs from the literature in that we exhibit, at a high level of abstraction, a new path for performing efficient quantitative information-flow analysis while keeping low inputs symbolic. In Sections 5 and 6 we instantiate this idea for the observers defined in Section 3.

4.1 Quantifying Leaks

As is common in quantitative information-flow analysis, we quantify amount of secret information leaked by a program in terms of the maximum number of observations an adversary can make, for any valuation of the low input. Formally, we define leakage as

$$\mathcal{L} := \max_{\lambda \in I_{lo}} (|\text{view}(\text{Col}_\lambda)|). \quad (1)$$

The logarithm of this number corresponds to the number of leaked *bits* w.r.t. different measures of entropy, and it comes with different interpretations in terms of security: For example, it can be related to a lower bound on the expected number of guesses an adversary has to make for successfully recovering the secret input [23], or to an upper bound for the probability of successfully guessing the secret input in one shot [33].

4.2 Static Bounds on Leaks, with Low Inputs

For quantifying leakage based on Equation 1, one needs to determine the size of the range of view applied to the fixpoint Col_λ of the next operator, for all $\lambda \in I_{lo}$ – which is infeasible for most programs. For *fixed* values $\lambda \in I_{lo}$, however, the fixpoint computation can be tractably approximated by abstract interpretation [10]. The result is a so-called abstract fixpoint Col^\sharp that represents a superset of Col_λ , based on which one can over-approximate the range of view [20].

The novelty in this paper is that we compute abstract fixpoints $\text{Col}^\sharp(s)$ that contain dedicated symbols s representing the unknown values of the low inputs. The core advantage of introducing symbols for representing low inputs is that it allows us to separate variations in observable outputs due to low inputs (which are unproblematic)

from those that are due to high inputs (which consist potential leaks). We describe our symbolic abstract domain in Section 5 before we sketch its soundness proof in Section 7.

5 Masked Symbol Abstract Domain

Cache-aware code often uses Boolean and arithmetic operations on pointers in order to achieve favorable memory alignment. In this section we devise the *masked symbol domain*, which is a simple abstract domain that enables the static binary analysis of such code in the presence of dynamically allocated memory.

5.1 Dynamic Memory as Low Data

Dynamic memory locations are not known at analysis time. To deal with them statically, we rely on the assumption that locations chosen by the allocator do not depend on secret data. More precisely, we assume that those locations are part of the low initial state, i.e., I_{lo} contains a pool of low heap locations that can be dynamically requested by the program.

5.2 Representation

The masked symbol domain is based on finite sets of what we call *masked symbols*, which are pairs (s, m, o) consisting of the following components: *symbol* $s \in \text{Sym}$, uniquely identifying an unknown value, such as a base address; a *mask* $m \in \{0, 1, \top\}^n$, representing a pattern of known and unknown bits; and an *offset* $o \in \{0, 1\}^n$, representing an offset from the unknown bits. The i -th bit of a masked symbol (s, m, o) is equal to $m_i \in \{0, 1\}$, unless $m_i = \top$, in which case it is unknown. In the first case we call the bit *masked*, in the second *symbolic*. We abbreviate the mask (\top, \dots, \top) by \top .

Two special cases are worth pointing out:

1. $(s, \top, 0)$ represents an unknown constant, and
2. $(s, m, 0)$ with $m \in \{0, 1\}^n$ represents the bit-vector m .

That is, pairs of the form (s, m, o) generalize both bitvectors and unknown constants.

5.3 Concretization and Counting

We now give a semantics to elements of the masked symbol domain. This semantics is parametrized w.r.t. instantiations of the symbols. For the case where masked symbols represent partially known heap addresses, a valuation corresponds to one specific layout.

Technically, we define the concretization of finite sets $F \subseteq \text{Sym} \times \{0, 1, \top\}^n \times \{0, 1\}^n$ w.r.t. a mapping

$\lambda : \text{Sym} \rightarrow \{0, 1\}^n$ taking symbols to bit-vectors:

$$\gamma_\lambda(F) = \{(\lambda(s) \odot m) + o \mid (s, m, o) \in F\}.$$

Here \odot is defined bitwise by $(\lambda(s))_i \odot m_i = m_i$ whenever $m_i \in \{0, 1\}$, and $(\lambda(s))_i$ otherwise. Modeling λ as a mapping from symbols to bitvectors is a natural generalization of the presentation in Section 4 to a low state consisting of multiple components that are represented by different symbols.

The following proposition shows that precise valuation of the constant symbols can sometimes be ignored for deriving upper bounds on the numbers of values that the novel domain represents. It enables the quantification of information leaks in the absence of exact information about locations on the heap. For this we note that a symbol s can be seen as a vector of symbols (s_{n-1}, \dots, s_0) , one per each bit. This allows the application of the adversary’s *view* (see Section 3) on masked symbols, as the respective projection to a subset of observable masked bits.

Proposition 1. *For every valuation $\lambda : \text{Sym} \rightarrow \{0, 1\}^n$ and every projection *view* mapping vectors to a subset of their components, we have $|\text{view}(\gamma_\lambda(F))| \leq |\text{view}(F)|$.*

Proposition 1 gives us a means to derive upper bounds on the range of the view of an adversary, for *any* valuation of the symbols.

Example 2. *The projection of the set $F = \{(s, (0, 0, 1), 0), (t, (\top, \top, 1), 0), (u, (1, 1, 1), 0)\}$ of (three bit) masked symbols to their two most significant bits yields the set $\{(0, 0), (t_2, t_1), (1, 1)\}$, i.e. we count three observations. However, the projection to their least significant bit yields only the singleton set $\{1\}$, i.e. the observation is determined by the masks alone. We use this observation for static reasoning about cache-aware memory alignment.*

5.4 Update

Next we describe the effect of interpreted x86 assembly instructions between pairs masked symbols. The lifting of those operations to sets of masked symbols is obtained by performing the operations on all elements in their product. This allows tracking information about known bits (which we encode in the mask) and about offsets from symbols.

5.4.1 Tracking Bits

An important class of operations for cache-aware coding are those that allow the alignment of data to memory blocks without knowing the precise pointer value.

Example 3. *The following code snippet is produced when compiling the `align` function from Figure 3 with `gcc -O2`. The register `EAX` contains a pointer to a dynamically allocated heap memory location.*

```
1      AND 0xFFFFFFFFC0, EAX
2      ADD 0x40, EAX
```

The first line ensures that the 6 least significant bits of that pointer are set to 0, thereby aligning it with cache lines of 64 bytes. The second line ensures that the resulting pointer points into the allocated region while keeping the alignment.

To reason about this kind of code, we define the bitwise effect of instructions considering three cases.

- (a) If the i -th bit of one operand is masked, in case that basic properties of the instructions reveal the exact resulting bit, store it in the mask. Such basic properties include: AND between symbolic and 0-bits reveals that the resulting bits are 0; OR between symbolic and 1-bits reveals that the resulting bits are 1; XOR between the same symbolic bits reveals that the resulting bits are 0. For example, when performing Line 1 in Example 3, assuming that `EAX` has the symbolic value $(s, \top, 0)$, results in a masked symbol

$$(s, (\top \dots \top 000000), 0). \quad (2)$$

- (b) If the i -th bit of one operand is masked and of the other operand is symbolic, in case that basic properties of the instructions reveal that the symbolic value is retained, keep the same symbolic bit in the result. Such basic properties include: AND between symbolic and 1-bits; OR between symbolic and 0-bits; AND or OR between the same symbolic bits. For example, the addition of `0x3F` to (2) results in a masked symbol

$$(s, (\top \dots \top 111111), 0), \quad (3)$$

for which we can statically determine containment in the same cache line as $(s, (\top \dots \top 000000), 0)$.

- (c) Otherwise, a fresh symbolic bit-value is stored. For example, the addition of `0x40` to (2) in Example 3 results in the masked symbol

$$(s', (\top \dots \top 000000), 0), \quad (4)$$

pointing to the beginning of some (unknown) cache line.

5.4.2 Tracking Offsets

We add support for tracking offsets from symbols, which is required to enable the analysis of low-level code.

Example 4. The loop in the `gather` function from Figure 3, which increments an index variable, is transformed to a loop doing pointer arithmetic on dynamically allocated memory locations, when compiled with `gcc -O2`. Corresponding pseudocode looks as follows:

```

1  y := r + N - 1
2  for x := r to y do
3      *x = buf [k + i * spacing]
```

There, r points to a dynamic memory location. The loop terminates whenever pointer x points at or beyond y .

The operations on masked symbols defined so far are not sufficient for a precise analysis of the code in Example 4, e.g. when r has a symbolic value $(s, \top, 0)$. In this case, y will be assigned a fresh symbolic value $(s', \top, 0)$, and at iteration $i = 2, 3, 4, \dots$ of the loop, x will be assigned a fresh symbolic value $(s_i, \top, 0)$. Without additional knowledge, the equality or inequality between s_i and s' cannot be determined, which prohibits determining at which iteration the loop is terminated.

To address this shortcoming, we add support for tracking offsets from symbols when interpreting addition between masked symbols. We remind the reader that the bit-wise definition of addition between x and y determines the i -th bit of the result as $r_i = x_i \oplus y_i \oplus c_i$, where c_i is the carry bit³. To determine the result of masked-symbol addition, we consider three cases.

- (a) If the i -th bit of one operand is masked, of the other operand is symbolic, and the carry bit is known, then the symbolic bit-value is retained, and the addition result is stored as an offset. For example, the variable y from Example 4 will obtain the value $(s, \top, r + N - 1)$, and at the i -th iteration of the loop, x will have the value (s, \top, i) . Returning to (4) in Section 5.4.1, the result will be set to $(s, (\top \dots \top 000000), 64)$.
- (b) If the i -th bits of the two operands are masked and the carry bit is known, then the exact bit-value of the addition result is stored in the mask, and the offset-bit is set to 0. This means that an offset is preferably encoded in the mask-bits and not in the offset-bits, as demonstrated in (3) in Section 5.4.1.
- (c) Otherwise, a fresh symbolic bit-value is stored. For example, addition between masked symbols $(s_1, \top, 0)$ and $(s_2, \top, 3)$, results in the fresh masked symbol $(s', \top, 0)$.

6 Memory Trace Abstract Domain

In this section, we present data structures for representing the set of possible memory accesses a program can

³The carry bit is defined as $c_0 = 0$ for the ADD instruction, c_0 is the carry flag for the ADC instruction, and $c_{i+1} = (x_i \wedge y_i) \vee (c_i \wedge x_i) \vee (c_i \wedge y_i)$.

make, and for computing the number of observations that different side channel attackers can make. For this we devise the *memory trace domains*, which capture the adversary models introduced in Section 3.2: address-trace (adversary who can observe addresses), block-trace (adversary who can observe memory blocks), and b-block-trace (adversary who can observe memory blocks modulo repetitions). We describe those domains, and elaborate on developments which allow us to precisely capture cases where a b-block-trace adversary learns less information than an address- and block-trace adversary, as is the case in the following example.

6.1 Representation

We use a directed acyclic graph (DAG) to compactly represent traces of memory accesses. While a DAG representation can precisely represent a set of traces [11], a counting procedure which does not require enumerating all traces may lose precision. The representation we devise is precise for the b-block observer, and provides an easy counting procedure.

The DAG has a set of nodes N representing memory accesses, with a root r and set of edges $E \subseteq N \times N$. We equip each node $n \in N$ with a label $L(n)$ that represents the adversary's view of the node (i.e. addresses or blocks), and a repetition count $R(n)$ that represents the number of times each address may be repeatedly accessed. We represent labels $L(n)$ using the masked symbols abstract domain (see Section 5), and use a finite set abstraction to represent $R(n)$.

6.2 Concretization and Counting

In a memory trace domain, each node n represents the set of traces of the program up to this point of the analysis. Its concretization function is defined by

$$\gamma(n) = \bigcup_{\substack{r=n_0 \dots n_k=n \text{ is a} \\ \text{path from } r \text{ to } n}} \{\ell_0^{\ell_0^k} \dots \ell_k^{\ell_k^k} \mid \ell_i \in L(n_i), t_i \in R(n_i)\},$$

that is, for every path in the graph, we collect the adversary's observations (given by the labels of its nodes) and their number (given by the repetition count).

For quantitatively assessing leaks we are interested in the number of observations $|\gamma(n)|$ an adversary can make. An upper bound on this number is easily computed from the memory trace domains using the recursive equation

$$cnt(n) = |R(n)| \cdot |L(n)| \cdot \sum_{(s,n) \in E} cnt(s) \quad (5)$$

For the b-block trace observer, we replace the factor $|R(n)|$ from the expression in (5) by 1, which captures

that this observer cannot distinguish between repetitions of accesses to the same memory block.

6.3 Update and Join

The memory trace domains are equipped with functions for update and join, which govern how sets of traces are extended and merged, respectively. The domains are defined with respect to an observer modeled by the $view \in \{view^{addr}, view^{block}, view^{bblock}\}$, for the different views introduced in Section 3. Below we overload the notation of $view$ to take as input sets of addresses, and return the respective set of observations (i.e. addresses or blocks).

The *update* receives a node n representing a set of traces of memory accesses, and it extends n by a new access to a potentially unknown address that represented a finite set of masked symbols F . Technically:

1. If the set of masked symbols is not a repetition (i.e. if $L(n) \neq view(F)$) the update function appends a new node n' to n (adding (n, n') to E) and it sets $L(n') = view(F)$ and $R(n') = \{1\}$.
2. Otherwise (i.e. if $L(n) = view(F)$) it increments the possible repetitions in $R(n)$ by one.

The *join* for two nodes n_1, n_2 first checks whether those nodes have the same parents and the same label, in which case n_1 is returned, and their repetitions are joined. Otherwise a new node n' with $L(n') = \{\varepsilon\}$ is generated and edges (n_1, n') and (n_2, n') are added to E .

To increase precision in counting for the b-block adversary, joins are delayed until the next update is performed. This captures cases where an if-then-else statement spans two memory blocks, both of which are accessed regardless whether if-condition is taken or not.

7 Soundness

In this section we outline how to establish the soundness of our approach; we will give the full proof details in an extended version of this paper. The novelty in our approach is that we aim to establish leakage bounds w.r.t. *all* valuations of low variables, requiring us to extend established notions of local and global soundness [10] as we explain below.

7.1 Global Soundness and Leakage Bounds

For the proof, we distinguish between the symbols in $Sym_{I_0} \subseteq Sym$ that represent the low initial state and those in $Sym \setminus Sym_{I_0}$ that are introduced during the analysis. A specific low initial state in I_0 is then given in terms of valuation of low symbols $\lambda : Sym_{I_0} \rightarrow \{0, 1\}^n$.

When introducing a fresh symbol s (see Section 5), we need to extend the domain of λ to include s . To this end, we denote by $Ext(\lambda)$ the set of all functions $\bar{\lambda}$ with $ran(\bar{\lambda}) = \{0, 1\}^n$ such that $dom(\lambda) \subseteq dom(\bar{\lambda}) \subseteq Sym$ and $\bar{\lambda} \upharpoonright_{dom(\lambda)} = \lambda$.

With this notation, we can express the *global soundness* of a symbolic fixpoint Col^\sharp as follows:

$$\forall \lambda \in I_0 \exists \bar{\lambda} \in Ext(\lambda) : Col_\lambda \subseteq \gamma_{\bar{\lambda}}(Col^\sharp). \quad (6)$$

Equation (6) ensures that every trace is included in a concretization of the symbolic fixpoint. Based on the soundness of the symbolic fixpoint, we can immediately define bounds for the leakage w.r.t. all low values.

$$\mathcal{L} \leq \max_{\lambda \in I_0} |view(\gamma_\lambda(Col^\sharp))| \quad (7)$$

Even though we do not explicitly track $\bar{\lambda}$, the *existence* of $\bar{\lambda}$ suffices for establishing the correctness of our quantitative analysis, as our counting procedures (see Section 5.3 and Section 6.2) allow the overapproximation of the right-hand side of Equation (7) for any $\bar{\lambda}$.

7.2 From Local Soundness to Global Soundness

An abstract domain is *locally sound* if the abstract transition function over-approximates the effect of the *next* operator (here: in terms of set inclusion):

$$\forall \lambda, \exists \bar{\lambda} \in Ext(\lambda), \forall a \in Col^\sharp : next(\gamma_\lambda(a)) \subseteq \gamma_{\bar{\lambda}}(next^\sharp(a))$$

It is a fundamental result from abstract interpretation [10] that local soundness implies global soundness. When the fixpoint is reached in a finite number of steps, we obtain this result for our modified notions of soundness, by induction on the number of steps. This is sufficient for the development in our paper; we leave an investigation of the general case to future work.

7.3 Local Soundness: Masked Symbols

To establish the local soundness of the masked symbol domain introduced in Section 5, we need to prove that the masked symbols obtained after the interpretation of the instructions AND, OR, ADD, etc., correctly overapproximate the result of the instructions for a valuation λ . For the cases resulting in a fresh symbol, the overapproximation holds because the fresh symbol may have any value, including the concrete result. In the remaining cases, the set inclusion holds due to basic properties of arithmetic operations such as $x \wedge 0 = 0$, $x \wedge 1 = x$, etc. A formal proof for the local soundness of the masked symbol domain will be given in an extended version of the paper.

7.4 Local Soundness: Memory Trace Domain

The local soundness of the memory trace domains follows directly because the update does not perform any abstraction with respect to the concrete trace of observations; it just yields a more compact representation in case of repetitions of the same observation.

8 Case Study

In this section, we present a case study which leverages the techniques developed in this paper for the first rigorous analysis of several countermeasures against cache side channel attacks against modular exponentiation algorithms from versions of libgcrypt and OpenSSL from April 2013 to March 2016. We report on results for leakage to the adversary models presented in Section 3.2 due to instruction-cache (I-cache) accesses and data-cache (D-cache) accesses.⁴ As the adversary models are ordered according to their observational capabilities, this sheds light into the level of provable security that different protections offer.

8.1 Tool building

We implement the novel abstract domains described in Sections 5 and 6 on top of the CacheAudit open source static analyzer [11]. CacheAudit provides infrastructure for parsing, control-flow reconstruction, and fixed point computation. Our novel domains extend the scope of CacheAudit by providing support for (1) the analysis of dynamically allocated memory, and for (2) adversaries who can make fine-grained observations about memory accesses. The resulting extensions to CacheAudit will be made publicly available.

8.2 Target Implementations

For libgcrypt we consider versions 1.5.2 to 1.6.3. In those versions of libgcrypt, four variants of modular exponentiation are implemented, with different protections against side-channel attacks. In addition to those implementations, we analyze two side-channel protections introduced in OpenSSL versions 1.0.2f and 1.0.2g, respectively. For cleaner comparison of security and performance we implement all protections on top of libgcrypt 1.6.3 and analyze this code instead.

To generate the target executables of our experiments, we use ElGamal decryption routines based on each of the

⁴We also analyzed the leakage from accesses to shared instruction- and data-caches; for the analyzed instances, the leakage results were consistently the maximum of the I-cache and D-cache leakage results.

above-described implementations of modular exponentiation and the respective countermeasures, resulting in 5 implementations. We compile them using GCC 4.8.4, on a 32-bit Linux machine running kernel 3.13. For ElGamal decryption, we use a key size of 3072 bits.

The current version of CacheAudit supports only a subset of the x86 instruction set, which we extended with instructions required for the case study. To bound the required extensions we focus our analysis on the regions of the executables that were targeted by exploits and to which the corresponding countermeasures were applied, rather than the whole executables. As a consequence, the formal statements we derive only hold for those regions. In particular, we do not analyze the code of the libgcrypt’s multi-precision integer multiplication and modulo routines, and we specify that the output of the memory allocation functions (e.g. `malloc`) is symbolic (see Section 5).

8.3 Square-and-Multiply Modular Exponentiation

The first target of our analysis is modular exponentiation by square-and-multiply. The algorithm is depicted in Figure 5 and is implemented, e.g., in libgcrypt version 1.5.2. Line 5 of the algorithm contains a conditional branch whose condition depends on a bit of the secret exponent. An attacker who can observe the victim’s accesses to instruction or data caches may learn which branch was taken and identify the value of the exponent bit. This weakness has been shown to be vulnerable to key-recovery attacks based on prime+probe [22, 39] and flush+reload [37].

In response to these attacks, libgcrypt 1.5.3 implements a countermeasure that makes sure that the squaring operation is always performed, see Figure 6 for the pseudocode. It is noticeable that this implementation still contains a conditional branch that depends on the bits of the exponent in Line 7, namely the copy operation that selects the outcome of both multiplication operations. However, this has been considered a minor problem because the branch is small and is expected to fit into the same cache line as preceding and following code, or to be always loaded in cache due to speculative execution [37]. In the following we apply the techniques developed in this paper to analyze whether the expectations on memory layout are met.

Results The results of our analysis are given in Figure 7 and Figure 9

- Our analysis identifies a 1-bit data cache leak in square-and-multiply exponentiation (line 2 in Figure 7a), due to memory accesses in the conditional branch in that implementation. Our analysis confirms that this data

```

1 r := 1
2 for i := |e| - 1 downto 0 do
3   r := mpi_sqr(r)
4   r := mpi_mod(r, m)
5   if e_i = 1 then
6     r := mpi_mul(b, r)
7     r := mpi_mod(r, m)
8   return r

```

Figure 5: Square-and-multiply modular exponentiation

```

1 r := 1
2 for i := |e| - 1 downto 0 do
3   r := mpi_sqr(r)
4   r := mpi_mod(r, m)
5   tmp := mpi_mul(b, r)
6   tmp := mpi_mod(tmp, m)
7   if e_i = 1 then
8     r := tmp
9   return r

```

Figure 6: Square-and-always-multiply exponentiation

Observer	address	block	b-block
I-Cache	1 bit	1 bit	1 bit
D-Cache	1 bit	1 bit	1 bit

(a) Square-and-multiply from libgcrypto 1.5.2

Observer	address	block	b-block
I-Cache	1 bit	1 bit	0 bit
D-Cache	0 bit	0 bit	0 bit

(b) Square-and-always-multiply from libgcrypto 1.5.3

Figure 7: Leakage of modular exponentiation algorithms to observers of instruction and data caches, with cache line size of 64 bytes and compiler optimization level $-O2$.

cache leak is closed by square-and-always-multiply (line 2 in Figure 7b).

- Line 1 of Figures 7a and Figure 7b show that both implementations leak through instruction cache to powerful adversaries who can see each access to the instruction cache. However, for weaker, b-block observers that cannot distinguish between repeated accesses to a block, square-and-always-multiply does *not* leak, confirming the intuition that the conditional copy operation is indeed less problematic than the conditional multiplication.

- The data in Figure 8 demonstrates that the advantages of conditional copy over conditional multiplication depend on details such as cache line size and compilation strategy. Figure 9 illustrates this effect for the conditional copy operation, where more aggressive compilation leads to more compact code that fits into single cache lines. The same effect is observable for data caches, where more aggressive compilation avoids data cache accesses altogether.

Observer	address	block	b-block
I-Cache	1 bit	1 bit	1 bit
D-Cache	1 bit	1 bit	1 bit

Figure 8: Leakage of square-and-always-multiply from libgcrypto 1.5.3, with cache line size of 32 bytes and compiler optimization level $-O0$.

```

41a80 8b 54 24 30 c1 e8 24 80 00 00 00
41a90 8b 84 24 80 00 00 00 85 c0 75 c6 89 e8 89 fd 89
41aa0 c7 83 ea 01 89 f0 d1 64 24 18 85 d2 0f 85 ef fe
41ab0 ff ff 83 6c 24 28 01 0f 89 d0 fe ff ff 89 c6 8b

```

(a) Compiled with the default gcc optimization level $-O2$. Regardless whether the jump is taken or not, first block 41a80 is accessed, followed by block 41aa0. This results in a 0-bit b-block leak.

```

5d040 8b 45 9c c1 e8 1f 89 c2 8b 85 24 80 00 00 00
5d050 8b 85 30 ff ff ff 89 45 d4 8b 45 94 89 85 50 ff
5d060 8b 85 30 ff ff ff 89 45 d4 8b 45 94 89 85 50 ff
5d070 ff ff 8b 45 d4 8b 45 94 8b 45 a0 89 85 48 ff ff
5d080 ff d1 65 9c 83 6d 98 01 83 7d 98 00 0f 85 fe fd
5d090 ff ff 83 6d 90 01 83 7d 90 00 79 0d 90 83 7d c4

```

(b) Compiled with gcc optimization level $-O0$. The memory block 5d060 is only accessed when the jump is taken. This results in a 1-bit b-block leak.

Figure 9: Layout of libgcrypto 1.5.3 executables with 32-byte memory blocks (black lines denote block boundaries). The highlighted code corresponds to the conditional branching in lines 7–8 in Figure 6. The red region corresponds to the executed instructions in the if-branch. The blue curve points to the jump target, where the jump is taken if the if-condition does not hold.

8.4 Windowed Modular Exponentiation

In this section we analyze windowed algorithms for modular exponentiation. These algorithms differ from algorithms based on square-and-multiply in that they process multiple exponent bits in one shot. For this they commonly rely on tables filled with pre-computed powers of the base. For example, libgcrypto 1.6.1 pre-computes 7 multi-precision integers and handles the power 1 in a branch, see Figure 10. For moduli of 3072 bits, each pre-computed value requires 384 bytes of storage which amounts to 6-7 memory blocks in architectures with cache lines of 64 bytes. Key-dependent accesses to those tables can be exploited for mounting cache side channel attacks [22].

We consider three countermeasures, which are commonly deployed to defend against this vulnerability. They have in common that they all *copy* the table entries instead of returning a pointer to the entry.

- The first countermeasure ensures that in the copy process, a constant sequence of memory locations is accessed, see Figure 11 for pseudocode. The expression on

```

1  if e0 == 0 then
2    base_u := bp
3    base_u_size := bsize
4  else
5    base_u := b_2i3[e0 - 1]
6    base_u_size := b_2i3size[e0 - 1]

```

Figure 10: Sliding window table lookup from libcrypt 1.6.1. Variable $e0$ represents the window, right-shifted by 1. The lookup returns a pointer to the first limb of the multi-precision integer in `base_u`, and the number of limbs in `base_u_size`. The first branch deals with powers of 1 by returning pointers to the base.

```

1  // Retrieves r from p[k]
2  secure_retrieve ( r , p , k):
3    for i := 0 to n - 1 do
4      for j := 0 to N - 1 do
5        v := p[i][j]
6        s := (i == k)
7        r[j] := r[j] ^ ((0 - s) & (r[j] ^ v))

```

Figure 11: A defensive routine for array lookup with a constant sequence of memory accesses, as implemented in libcrypt 1.6.3.

line 7 ensures that only the k -th pre-computed value is actually copied to r . This countermeasure is implemented, e.g. in NaCl and libcrypt 1.6.3.

- The second countermeasure stores pre-computed values in such a way that the i -th byte of all pre-computed values reside in the same memory block. This ensures that when the pre-computed values are retrieved, a constant sequence of memory blocks will be accessed. This so-called scatter/gather technique is described in detail in Section 2, with code in Fig 3, and is deployed, e.g. in OpenSSL 1.0.2f.

- The third countermeasure is a variation of scatter/gather, and ensures that the gather-procedure performs a constant sequence of memory accesses (see Figure 12). This countermeasure was recently introduced in OpenSSL 1.0.2g, as a response to the CacheBleed attack.

```

1  defensive_gather ( r , buf , k ):
2    for i := 0 to N-1 do
3      r[i] := 0
4      for j:= 0 to spacing - 1 do
5        v := buf[j + i*spacing]
6        s := (k == j)
7        r[i] := r[i] | (v & (0 - s))

```

Figure 12: A defensive implementation of gather (compare to Figure 3) from OpenSSL 1.0.2g.

Results Our analysis of the different versions of the table lookup yields the following results:⁵

Observer	address	block	b-block
I-Cache	1 bit	1 bit	1 bit
D-Cache	5.6 bit	2.3 bit	2.3 bit

(a) Leakage of secret-dependent table lookup in the modular exponentiation implementation from libcrypt 1.6.1.

Observer	address	block	b-block
I-Cache	0 bit	0 bit	0 bit
D-Cache	0 bit	0 bit	0 bit

(b) Leakage in the patch from libcrypt 1.6.3.

Observer	address	block	b-block
I-Cache	0 bit	0 bit	0 bit
D-Cache	1152 bit	0 bit	0 bit

(c) Leakage in the scatter/gather technique, applied to libcrypt 1.6.1.

Observer	address	block	b-block
I-Cache	0 bit	0 bit	0 bit
D-Cache	0 bit	0 bit	0 bit

(d) Leakage in the defensive gather technique from OpenSSL 1.0.2g, applied to libcrypt 1.6.1.

Figure 13: Instruction and data cache leaks of different table lookup implementations. Note that the leakage in Fig 13a accounts for copying a pointer, whereas the leakage in Fig 13b and 13c refers to copying multi-precision integers.

- Figure 13a shows the results of the analysis of the unprotected table lookup of Figure 10. The leakage of one bit for most adversaries is explained by the fact that they can observe which branch is taken. The layout of the conditional branch is demonstrated in Figure 14a; lowering the optimization level results in a different layout (see Figure 14b), and in this case our analysis shows that the I-Cache b-block leak is eliminated.

- More powerful adversaries that can see the exact address can learn $\log_2 7 = 2.8$ bits per access. The static analysis is not precise enough to determine that the lookups are correlated, hence it reports that at most 5.6 bits are leaked.

- Figure 13b shows that the defensive copying strategy from libcrypt 1.6.3 (see Figure 11) eliminates all leakage to the cache.

- Figure 13c shows that the scatter/gather copying-strategy eliminates leakage for any adversary that can observe memory accesses at the granularity of memory blocks, and this constitutes the first proof of security of this countermeasure. For adversaries that can see the full address-trace, our analysis reports a 3 bit leakage for each memory access, which is again accumulated over

⁵We note sliding window exponentiation exhibits further control-flow vulnerabilities, some of which we also analyze. To avoid redundancy with Section 8.3, we focus the presentation of our results on the lookup-table management.

```

4b980  8B 84 24 08 00 00 00 83 EE 01 89 84 24 94 00 00
4b990  00 75 je 4BA58 80 89 6C 24 44 8B 54 24 48 83
4b9a0  E2 0F 0F 84 B0 00 06 06 8D 4A FF 8B 94 8C B8 00
4b9b0  00 00 8B 8C 8C F4 00 00 00 8B 74 24 24 89 44 24
4b9c0  04 8B 44 24 40 89 54 24 03 8B 54 24 28 89 4C 24
4b9d0  0C 89 74 24 18 8B 74 24 1C 89 04 24 8B 44 24 44
4b9e0  89 74 24 14 8B 74 24 20 89 74 24 10 E8 CF F6 FF
4b9f0  FF 8B 84 24 98 00 06 06 89 84 24 94 00 00 00 E9
4ba00  84 FE FF FF 8D 74 26 03 83 6C 24 3C 01 0F 88 7B
4ba10  03 00 00 BF 20 00 00 00 8B 6C 24 3C 2B 7C 24 34
4ba20  89 FA 8B 7C 24 58 80 0C 16 89 54 24 38 89 4C 24
4ba30  30 8B 3C AF 8B 6C 24 2C 89 FA D3 EA 0F B6 4C 24
4ba40  38 D3 ED 8B 4C 24 34 99 EA 29 F1 D3 E7 89 7C 24
4ba50  2C E9 B5 FE FF FF 66 90 8B 4C 24 4C 8B 54 24 54
4ba60  E9 54 FF FF FF 8B 74 24 44 8B 54 24 40 89 74 24
4ba70  40 8D B4 24 98 00 00 00 89 54 24 44 89 74 24 28

```

(a) Compiled with the default gcc optimization level `-O2`. If the jump is taken, first block `4b980`, followed by block `4ba40`, followed by `4b980` again. If the branch is not taken, only block `4b980` is accessed.

```

47dc0  6C F6 FF FF 8B 84 24 98 00 00 00 89 84 24 94 00
47dd0  00 00 83 FF 01 74 14 09 F0 89 EE 89 C5 EB A9 89
47de0  E8 8B 6C je 47E0B 4 3C EB 04 89 74 24 3C 8B
47df0  54 24 44 83 E2 0F 74 13 83 EA 01 8B 84 94 B8 00
47e00  00 00 8B 94 94 F4 00 00 00 00 00 8B 54 24 50 8B
47e10  44 24 58 8D 8C 24 9C 00 00 00 89 4C 24 18 8B 7C
47e20  24 1C 89 7C 24 14 8B 7C 24 20 89 7C 24 10 89 54
47e30  24 0C 89 44 24 08 8B 84 24 94 00 00 00 89 44 24

```

(b) Compiled with gcc optimization level `-O1`. Regardless whether the jump is taken or not, first block `47dc0` is accessed, followed by block `47e00`.

Figure 14: Layout of executables using libgcrypt 1.6.1. The highlighted code corresponds to a conditional branch (blue: if-branch, red: else-branch). Curves represent jump targets.

correlated lookups because of imprecisions in the static analysis.

- The leak leading to the CacheBleed attack against scatter/gather [38] is visible when comparing the results of the analysis in Figure 13c with respect to address-trace and block-trace adversaries, however, its severity may be over-estimated due to the powerful address-trace observer. For a more accurate analysis of this threat, repeat the analysis for the bank-trace D-cache observer. The analysis results in 384-bit leak, which corresponds to one bit leak per memory access, accumulated for each accessed byte due to analysis imprecision (see above). The one bit leak in the i -th memory access is explained by the ability of this observer to distinguish between the two banks within which the i -th byte of all pre-computed values fall.

- Figure 13d shows that defensive gather from OpenSSL 1.0.2g (see Figure 12) eliminates all leakage to cache.

8.5 Discussion

A number of comments are in order when interpreting the bounds delivered by our analysis.

Use of Upper Bounds The results we obtain are upper bounds on the leaked information that are not necessarily tight, that is, they may be pessimistic. This means that while results of zero leakage corresponds to a proof of absence of leaks, positive leakage bounds do not correspond to proofs of the presence of leaks. The reason for this is that the amount of leaked information may be over-estimated due to imprecision of the static analysis, as is the case with the D-Cache leak shown on Figure 13c.

Use of Imperfect Models The guarantees we deliver are only valid to the extent to which the models used accurately capture the aspects of the execution platform relevant to known attacks. A recent empirical study of OS-level side channels on different platforms [7] shows that advanced microarchitectural features may interfere with the cache, which may render countermeasures ineffective.

Alternative Attack Targets In our analysis, we assume that heap addresses returned by malloc are low values. There are scenarios in which the heap addresses themselves are the target of cache attacks, e.g. when the goal is to reduce the entropy of ASLR [18].

8.6 Performance

We conclude the case study by considering the effect of the different countermeasures on the performance of modular exponentiation. For this, we use libgcrypt 1.6.3 as a base, and compile it with different versions of `mod_exp.c`, corresponding to each of the considered variants. We measure performance as the clock count (through the `rdtsc` instruction), as well as the number of performed instructions (through the `PAPI` library [26]), for performing exponentiations, for a sample of random bases and exponents. We make 100,000 measurements with an Intel Q9550 CPU.

Figure 15a summarizes our measurements. The results show that the applied countermeasure for square and multiply causes a significant slow-down of the exponentiation. A smaller slow-down is observed with sliding-window countermeasures as well; this slow-down is demonstrated in Figure 15b, which shows the performance of the retrieval of pre-computed values, with different countermeasures applied.

algorithm	square and multiply		sliding window			
	no CM	always multiply	no CM	scatter/gather	access all bytes	defensive gather
countermeasure (CM)						
implementation	libgcrypt 1.5.2	libgcrypt 1.5.3	libgcrypt 1.6.1	openssl 1.0.2f	libgcrypt 1.6.3	openssl 1.0.2g
instructions ($\times 10^6$)	90.32	120.62	73.99	74.21	74.61	75.29
cycles ($\times 10^6$)	75.58	100.73	61.58	61.65	62.20	62.28

(a) Different versions of modular exponentiation.

algorithm	sliding window		
	scatter/gather	access all bytes	defensive gather
countermeasure			
implementation	openssl 1.0.2f	libgcrypt 1.6.3	openssl 1.0.2g
instructions	2991	8618	13040
cycles	859	3073	5579

(b) Only multi-precision-integer retrieval step.

Figure 15: Performance measurements for libgcrypt 1.6.3 ElGamal decryption, for 3072-bit keys.

9 Related Work

Agat proposes a program transformation for removing control-flow timing leaks by equalizing branches of conditionals with secret guards [2], which he augments with an informal discussion of the effect of instruction and data caches [3]. Hedin and Sands [16] extend this timing model with execution histories, offering a hook for formal reasoning about cache state. Our approach relies on lower-level models, namely x86 executables and simple but accurate cache models, based on which we can perform an automatic analysis.

Molnar et al. [25] propose a program transformation that eliminates branches on secret to remove leaks due to control flow and instruction caches, together with a static check for the resulting x86 executables. Our approach is more permissive than theirs that it can establish the security of code that contains restricted forms of secret-dependent control flow and memory access patterns. It is worth emphasizing that the increased permissiveness of our approach comes from the fact that we rely on models of the hardware architecture for our analysis. If no such models are available, the safe way to go is to forbid all kinds of secret-dependent behavior.

Coppens et al. [8] investigate mitigations for timing-based side channels on x86 architecture, and they identify new side channels in programs without secret-dependent memory lookups due to out-of-order execution. In contrast, we prove the security of countermeasures. For this we rely on accurate models of caches, but we do not take into account out-of-order execution.

Langley [21] shows how to perform a dynamic analysis based on Valgrind, and this technique flags the secret-dependent (but cache-line independent) memory lookups of the OpenSSL sliding window-based modular exponentiation as a potential leak. Our technique gives more fine-grained insights about its security, including proofs

of security for adversaries that can observe memory accesses only at the granularity of memory blocks. Rodrigues et al. [31] develop a static analyzer reporting violations to constant-time coding practices in cryptographic implementations.

Technically, our work draws on methods from quantitative information-flow analysis (QIF) [6], where the automation by reduction to counting problems appears in [4, 27, 17, 24]. Specifically, our work builds on the CacheAudit tool [11], but goes beyond it in that it supports symbolic reasoning about dynamic memory allocation and wide variety of new adversary models.

Two existing approaches for quantifying leaks support symbolic reasoning about low inputs: [4] and [9] based logical operations on path formulas. In contrast, we introduce support for symbolic treatment of low inputs in an abstract interpretation framework for x86 executables.

10 Conclusions

In this paper we devise novel techniques that provide support for bit-level and arithmetic reasoning about pointers in the presence of dynamic memory allocation. These techniques enable us to perform the first rigorous analysis of widely deployed software countermeasures against cache side-channel attacks on modular exponentiation, based on executable code.

References

- [1] O. Aci mez, W. Schindler, and  . K. Ko . Cache based remote timing attack on the AES. In *CT-RSA*, pages 271–286. Springer, 2007.
- [2] J. Agat. Transforming out timing leaks. In *POPL 2000*, pages 40–53. ACM, 2000.

- [3] J. Agat. Transforming out timing leaks in practice: An experiment in implementing programming language-based methods for confidentiality, 2000.
- [4] M. Backes, B. Köpf, and A. Rybalchenko. Automatic discovery and quantification of information leaks. In *SSP*, pages 141–153. IEEE, 2009.
- [5] D. Bernstein. Cache-timing attacks on AES, 2005.
- [6] D. Clark, S. Hunt, and P. Malacaria. A static analysis for quantifying information flow in a simple imperative language. *JCS*, 15(3):321–371, 2007.
- [7] D. Cock, Q. Ge, T. Murray, and G. Heiser. The last mile: An empirical study of timing channels on sel4. In *CCS*. ACM, 2014.
- [8] B. Coppens, I. Verbauwhede, K. D. Bosschere, and B. D. Sutter. Practical mitigations for timing-based side-channel attacks on modern x86 processors. In *SSP*, pages 45–60. IEEE, 2009.
- [9] P. M. Corina Pasareanu, Sang Phan. Multi-run side-channel analysis using symbolic execution and max-smt. In *CSF*. IEEE, 2016.
- [10] P. Cousot and R. Cousot. Abstract interpretation: a unified lattice model for static analysis of programs by construction of approximation of fixpoints. In *POPL*, pages 238–252, 1977.
- [11] G. Doychev, B. Köpf, L. Mauborgne, and J. Reineke. Cacheaudit: A tool for the static analysis of cache side channels. *ACM Transactions on Information and System Security*, 18(1):4:1–4:32, June 2015.
- [12] S. Dziembowski and K. Pietrzak. Leakage-resilient cryptography. In *FOCS*. IEEE, 2008.
- [13] Ú. Erlingsson and M. Abadi. Operating system protection against side-channel attacks that exploit memory latency. Technical report, 2007.
- [14] S. Gueron. Intel Advanced Encryption Standard (AES) Instructions Set. <http://software.intel.com/file/24917>, 2010.
- [15] D. Gullasch, E. Bangerter, and S. Krenn. Cache games - bringing access-based cache attacks on AES to practice. In *SSP*, pages 490–505. IEEE, 2011.
- [16] D. Hedin and D. Sands. Timing aware information flow security for a JavaCard-like bytecode. *ENTCS*, 141(1):163–182, 2005.
- [17] J. Heusser and P. Malacaria. Quantifying information leaks in software. In *ACSAC*, pages 261–269. ACM, 2010.
- [18] R. Hund, C. Willems, and T. Holz. Practical timing side channel attacks against kernel space aslr. In *Security and Privacy (SP), 2013 IEEE Symposium on*, pages 191–205. IEEE, 2013.
- [19] T. Kim, M. Peinado, and G. Mainar-Ruiz. StealthMem: System-level protection against cache-based side channel attacks in the cloud. In *19th USENIX Security Symposium*. USENIX, 2012.
- [20] B. Köpf and A. Rybalchenko. Approximation and randomization for quantitative information-flow analysis. In *CSF*, pages 3–14. IEEE, 2010.
- [21] A. Langley. Checking that functions are constant time with valgrind. <https://www.imperialviolet.org/2010/04/01/ctgrind.html>, 2010. Accessed: 6 March 2016.
- [22] F. Liu, Y. Yarom, Q. Ge, G. Heiser, and R. B. Lee. Last-level cache side-channel attacks are practical. In *IEEE Symposium on Security and Privacy*, pages 605–622. IEEE Computer Society, 2015.
- [23] J. L. Massey. Guessing and Entropy. In *ISIT*, page 204. IEEE, 1994.
- [24] Z. Meng and G. Smith. Calculating bounds on information leakage using two-bit patterns. In *PLAS*. ACM, 2011.
- [25] D. Molnar, M. Piotrowski, D. Schultz, and D. Wagner. The program counter security model: Automatic detection and removal of control-flow side channel attacks. In *ICISC*. Springer, 2006.
- [26] P. J. Mucci, S. Browne, C. Deane, and G. Ho. Papi: A portable interface to hardware performance counters. In *DoD HPCMP Users Group Conference*, 1999.
- [27] J. Newsome, S. McCamant, and D. Song. Measuring channel capacity to distinguish undue influence. In *PLAS*, pages 73–85. ACM, 2009.
- [28] D. A. Osvik, A. Shamir, and E. Tromer. Cache attacks and countermeasures: the case of AES. In *CT-RSA*, volume 3860 of *LNCS*, pages 1–20. Springer, 2006.
- [29] C. Percival. Cache missing for fun and profit. In *BSDCan*, 2005.
- [30] T. Ristenpart, E. Tromer, H. Shacham, and S. Savage. Hey, you, get off of my cloud: exploring information leakage in third-party compute clouds. In *CCS*, pages 199–212. ACM, 2009.
- [31] B. Rodrigues, F. M. Quintão Pereira, and D. F. Aranha. Sparse representation of implicit flows with applications to side-channel detection. In *Proceedings of the 25th International Conference on Compiler Construction*, pages 110–120. ACM, 2016.
- [32] S. Shinde, Z. L. Chua, V. Narayanan, and P. Saxena. Preventing page faults from telling your secrets. In *ASIACCS*. ACM, 2016.
- [33] G. Smith. On the foundations of quantitative information flow. In *FoSSaCS*. Springer, 2009.
- [34] M. Tiwari, J. Oberg, X. Li, J. Valamehr, T. E. Levin, B. Hardekopf, R. Kastner, F. T. Chong, and T. Sherwood. Crafting a usable microkernel, processor, and I/O system with strict and provable information flow security. In *ISCA*, pages 189–200. ACM, 2011.
- [35] Z. Wang and R. B. Lee. A novel cache architecture with enhanced performance and security. In *MICRO*, 2008.
- [36] Y. Xu, W. Cui, and M. Peinado. Controlled-channel attacks: Deterministic side channels for untrusted operating systems. In *SSP*. IEEE, 2015.

- [37] Y. Yarom and K. Falkner. FLUSH+RELOAD: A high resolution, low noise, L3 cache side-channel attack. In *USENIX Security Symposium*, 2014.
- [38] Y. Yarom, D. Genkin, and N. Heninger. Cachebleed: A timing attack on openssl constant time rsa. Cryptology ePrint Archive, Report 2016/224, March 2016. <http://eprint.iacr.org/>.
- [39] Y. Zhang, A. Juels, M. K. Reiter, and T. Ristenpart. Cross-VM side channels and their use to extract private keys. In *CCS*. ACM, 2012.
- [40] Y. Zhang and M. K. Reiter. Düppel: retrofitting commodity operating systems to mitigate cache side channels in the cloud. In *Proceedings of the 2013 ACM SIGSAC conference on Computer & communications security*, pages 827–838. ACM, 2013.